

the lipophilicity of the viologen increases the charge separation yield as a result of a decrease in the back electron transfer rate.⁶³ This same explanation accounts for the present results. Both ESE and ENDOR indicate that the longer chain length (or more lipophilic) viologens are solubilized deeper into the vesicle bilayer, which correlates with an increase in the net photoreduction yield of the radical (Figures 1 and 2).

For alkylviologens solubilized in cationic vesicles, the photoreduction yield is consistently higher than in anionic DHP,²⁵ which indicates that lowering the barrier to electron transfer increases the net photoreduction yield. Adding cholesterol to the DHP vesicle also increases the photoreduction yield (Figure 3). The ESE and ENDOR results suggest that added cholesterol disrupts the interface of the vesicle. Since the cholesterol intercalates between the headgroups of the vesicle lowering the effective surface charge density, the barrier to electron transfer is reduced, which results in an increased photoreduction yield. All of the alkylviologens show a growth in photoreduction yield with an increase in the cholesterol concentration up to 23 mol % (Figure 3). At 33 mol % cholesterol, there is little further change in the photoreduction yield. The ESE results in Figure 5 show that at 33 mol % the modulation depths for the alkylviologens increase and converge to the same approximate value. The photoreduction yield and ESE results together suggest that, at 33 mol % cholesterol, the interface is well hydrated and is no longer as effective in lowering the rate of back electron transfer. The ESE and ENDOR data show that MV²⁺ remains at the vesicle interface with increasing cholesterol concentrations; therefore, lowering the barrier

to electron transfer by reducing the surface charge density through addition of cholesterol does not affect the photoreduction yield of MV²⁺.

Conclusions

The effect of alkyl chain length on the photoreduction of a series of alkylviologens solubilized in DHP vesicles with and without added cholesterol was evaluated by ESR, ESEM, and ENDOR. The ESE and ENDOR data show that the longer chained viologens are located deeper into the vesicle. The integrated ESR intensity shows an increase in the photoreduction yield with increasing alkyl chain length of the alkylviologen. This correlation is interpreted as a reduction in the rate of back electron transfer through the anionic interface as the alkyl chain length is increased. Addition of cholesterol to the vesicle results in an increase in the photoreduction yield of the radical. ESEM patterns show that adding cholesterol causes increased water penetration into the interface. The ENDOR results indicate that the effective proton density in the interface region is reduced as cholesterol intercalates into the bilayer. A probable interpretation of the photoreduction yield increase is that added cholesterol reduces the effective interface charge density which lowers the barrier for electron transfer between the chloride counterion and the alkylviologen moiety.

Acknowledgment. This research was funded by the Division of Chemical Sciences, Office of Basic Energy Research, Office of Energy Research, U.S. Department of Energy. We thank D. H. P. Thompson and J. K. Hurst for the AV²⁺ compounds.

Registry No. DHP, 2197-63-9; MV²⁺, 1910-42-5; C₆V²⁺, 116911-79-6; C₈V²⁺, 116911-80-9; C₁₂V²⁺, 74733-79-2; C₁₆V²⁺, 75805-30-0; cholesterol, 57-88-5.

(63) Schmehl, R.; Whitten, D. G. *J. Phys. Chem.* 1981, 85, 3473.

Location and Photolization Studies of a Series of Alkylporphyrin Derivatives Solubilized in Dioctadecyldimethylammonium Chloride and Dihexadecyl Phosphate Vesicles

Emmanuelle Chastenet de Castaing and Larry Kevan*

Department of Chemistry, University of Houston, Houston, Texas 77204-5641 (Received: May 29, 1991; In Final Form: August 5, 1991)

Three alkylporphyrins were synthesized, 5-(1-nonylpyridinium-4-yl)-10,15,20-triphenylporphyrin bromide (H₂PC₉), 5-(1-dodecylpyridinium-4-yl)-10,15,20-triphenylporphyrin bromide (H₂PC₁₂), and 5-(1-hexadecylpyridinium-4-yl)-10,15,20-triphenylporphyrin bromide (H₂PC₁₆). The location of these 5-(1-alkylpyridinium-4-yl)-10,15,20-triphenylporphyrin bromides (H₂PC_n) solubilized in cationic dioctadecyldimethylammonium chloride (DODAC) and anionic dihexadecyl phosphate (DHP) vesicles solutions was investigated using optical absorption spectroscopy. Electron spin resonance (ESR) was applied to observe the yields of photoionization of H₂PC_n in rapidly frozen DODAC and DHP vesicle solutions versus alkyl chain length. A decrease in photoyield correlated with an increase in the porphyrin-to-vesicle interface distance. The photoionization of H₂PC_n in rapidly frozen DODAC and DHP vesicle solutions containing electron acceptors was also studied by ESR. Two different electron acceptors were used in this study, tetrabromobenzoquinone (TBBQ) and potassium ferricyanide (K₃Fe(CN)₆). Electron transfer within the vesicle itself was examined with TBBQ, which solubilizes inside the lipophilic region of the vesicle near the interface, whereas K₃Fe(CN)₆ involved electron transfer across the vesicle interface. The yields of photoionization of H₂PC_n have generally been found to decrease upon addition of either acceptor. The results are discussed in terms of alkyl chain length, position of the porphyrin group relative to the vesicle interface, and vesicle surface charge.

Introduction

Light-induced electron transfer reactions in micelles and vesicles solutions have been extensively investigated with the aim of optimizing the net conversion of light energy into chemical energy.¹⁻⁴

The efficiency of photoinduced net charge separation is known to depend on structural factors of the surfactant assemblies, such as their size,⁵ their surface charge density,⁶ or the amount of hydration at their surface.^{7,8} Another important factor is the

(1) Calvin, M. In *Photochemical Conversion and Storage of Solar Energy*; Connolly, J. S., Ed.; Academic: New York, 1981; Chapter 1.

(2) Balzani, V. In *Photochemical Conversion and Storage of Solar Energy*; Connolly, J. S., Ed.; Academic: New York, 1981; Chapter 4.

(3) Kevan, L. In *Photoinduced Electron Transfer, Part B*; Fox, M. A., Chanon, M., Eds.; Elsevier: Amsterdam, 1988; p 329.

(4) Kalyanasundaram, K. *Photochemistry in Microheterogeneous Systems*; Academic: New York, 1987.

(5) Hiff, T.; Kevan, L. *J. Phys. Chem.* 1988, 92, 3982.

(6) Narayana, P. A.; Li, A. S. W.; Kevan, L. *J. Am. Chem. Soc.* 1982, 104, 6502.

(7) Ford, W. E.; Tollin, G. *Photochem. Photobiol.* 1984, 40, 249.

(8) Hiromitsu, I.; Kevan, L. *J. Am. Chem. Soc.* 1987, 109, 4501.

location of the donor and acceptor in the surfactant relative to the solvent, usually water.⁹ The ability of vesicles to localize molecules in definite sites according to intrinsic properties such as polarity can be used to control the spatial arrangement of donor/acceptor couples.^{9,10} In previous work, location of an additive solubilized in micelles or vesicles has been controlled by adding an alkyl chain to the solute.¹¹⁻¹⁶

Optical absorption spectroscopy has been used to determine the location of zinc tetraphenylporphyrin (ZnTPP) in reverse micelles¹⁷ and in vesicles.¹⁸ The location of electron donors has also been investigated by electron spin resonance (ESR) since the yield of photoirradiation generally depends on the strength of the photoproduct cation-water interaction.^{11,19,20} The quenching of the photoexcited state of an electron donor by an electron acceptor which is specifically localized in vesicle solutions is a way to gain further insight as to the location of the donor inside the vesicle. For example, tetrabromobenzoquinone (TBBQ) solubilizes inside the hydrocarbon core of the vesicle near the interface,²¹ whereas ferricyanide ions have a high charge density and do not penetrate the lipid bilayer and so solubilize at the interfaces of the vesicle. The quenching should enhance the photoionization efficiency, unless the electron acceptor is located too close to the porphyrin, in which case back electron transfer can occur to decrease the photoionization efficiency.

In the present study, a series of alkylporphyrin derivatives, H₂PC_n (*n* = 9, 12, and 16) is investigated to explore the effect of variable-length alkyl chains. The location of these alkylporphyrins solubilized in anionic and cationic vesicle solutions is investigated using optical absorption spectroscopy, and photoyields are investigated by ESR in the absence and presence of added electron acceptors. Alkyl chain length effects are observed which depend on electrostatic effects between the charged vesicle surfaces and the cationic porphyrins.

Experimental Section

Materials. The following alkylporphyrins (H₂PC_n) were prepared by alkylation of *meso*-triphenylpyridylporphyrin (H₂TTPPyP): 5-(1-nonylpyridinium-4-yl)-10,15,20-triphenylporphyrin bromide (H₂PC₉), 5-(1-dodecylpyridinium-4-yl)-10,15,20-triphenylporphyrin bromide (H₂PC₁₂), and 5-(1-hexadecylpyridinium-4-yl)-10,15,20-triphenylporphyrin bromide (H₂PC₁₆).

Benzaldehyde, 4-pyridinecarboxaldehyde, pyrrole, ethylene glycol, and the alkyl bromides were purchased from Aldrich. All the solvents were obtained from either Mallinckrodt or Baker. All chemicals were used without further purification except for pyrrole, which was freshly distilled, and DMF, which was distilled over molecular sieves (Grade 514 GT, 4 Å, from Mallinckrodt). Gravity column chromatography was performed on silica gel 62 (60–200 mesh), from Mallinckrodt, or on alumina neutral Brockman activity I, from Fisher. Thin-layer chromatography (TLC) plates of basic alumina and silica were purchased from Fisher; 300-MHz ¹H NMR spectra were recorded on a General Electric QE-300 spectrometer, at room temperature in deuterated chloroform (CDCl₃) solution. Absorption spectra were obtained

on a Perkin-Elmer Model 330 spectrophotometer with a 1-cm path length quartz cell.

H₂TTPPyP. A mixture of benzaldehyde (7 mL, 69 × 10⁻³ mol) and 4-pyridinecarboxaldehyde (3 mL, 31.5 × 10⁻³ mol) was added dropwise to 250 mL of refluxing propionic acid (173 °C), followed by freshly distilled pyrrole (6.25 mL, 0.09 mol). After reflux with strong magnetic stirring for 1.5 h, the reaction mixture was cooled to 90 °C. Ethylene glycol (175 mL) was added to induce precipitation of the porphyrin, and the reaction mixture was allowed to stand overnight in a refrigerator. The solution was then filtered, and a purple crystalline product was collected and washed with an ethanol/methanol mixture (50/50 v/v), and then with hexane. This crude product (3.1 g) was a mixture of *meso*-tetraphenylporphyrin (H₂TPP), H₂TTPPyP, and other tetraarylporphyrins.²² H₂TTPPyP was isolated and purified using gravity column chromatography. The crude product was dissolved in hot chloroform and then passed through alumina. The two fastest fractions, H₂TPP (*R_f* = 0.96) and H₂TTPPyP (*R_f* = 0.85), were collected and combined. They were chromatographed on silica gel in order to isolate H₂TTPPyP (*R_f* = 0.3) from H₂TPP (*R_f* = 1). Then, H₂TTPPyP was passed again through alumina. Further purification by recrystallization in chloroform/methanol, and finally drying at 50 °C in vacuo over phosphorus pentoxide led to 1.45 g (7%) of pure H₂TTPPyP. The compound was stored over P₂O₅ and under argon, until later use.

H₂PC_n with *n* = 9, 12, and 16. The alkylation of H₂TTPPyP to H₂PC_n was performed using a procedure derived from the alkylation of *meso*-tetrapyrrolylporphyrin described by Okuno.²³ H₂TTPPyP (100 mg, 0.16 mmol) and the appropriate alkyl bromide (6.5 mmol) were added to 100 mL of DMF. The solution was heated to boiling under reflux for 4 h under nitrogen. After removal of the solvent, the residue was washed several times with ethyl ether to eliminate the unreacted alkyl bromide. The resulting crude H₂PC_n was purified by gravity column chromatography on alumina. H₂PC₁₆, H₂PC₁₂, and H₂PC₉ were eluted with chloroform, chloroform/methanol (99/1 v/v), and chloroform/methanol (98/2 v/v), respectively. After evaporation of the solvent, the product was recrystallized from methanol/ether and dried at 50 °C in vacuum over phosphorus pentoxide. Pure purple crystals of H₂PC_n were collected in the following amounts: H₂PC₁₆ (90 mg, 61%), H₂PC₁₂ (105 mg, 76%), and H₂PC₉ (96 mg, 73%). The compounds were stored over P₂O₅ and under argon, until later use. They were identified by ¹H NMR and absorption spectroscopy. The spectroscopic data are consistent with the assigned structures and with the data reported in the literature for H₂PC₁₆.²²

Vesicles. DODAC was prepared from its bromide analogue (DODAB), which was passed through an ion-exchange resin.²⁴ DHP from Aldrich, tris(hydroxymethyl)aminomethane (Tris), gold label, 99.9+% from Aldrich, TBBQ from Alfa, and K₃Fe(CN)₆ from Fisher were used without further purification. Chloroform from Aldrich was HPLC grade. Water was deionized with a millipore/milli-Q system and had a resistivity greater than 18 MΩ-cm. Stock solutions of alkylporphyrin and of surfactant were prepared in chloroform with concentrations of 2 and 10 mM, respectively. These solutions were used within 48 h.

DODAC and DHP vesicle solutions were prepared so that the final surfactant concentration was 10 mM and the porphyrin concentration was 0–1.5 mM. DODAC vesicle solutions containing alkylporphyrin were prepared as follows: A measured volume of porphyrin solution, calculated to give the final desired porphyrin concentration, was mixed in a centrifuge tube with 1 mL of DODAC solution. A thin film of porphyrin/DODAC was formed on the wall of the tube by evaporation of the chloroform under a flow of nitrogen. Then 1 mL of deionized water was added to the thin film. The tube was shaken and gently warmed in a hot water bath (55 °C) until both the DODAC and the porphyrin were uniformly dissolved. The resulting viscous solution was

(9) Kevan, L. *Intl. Rev. Phys. Chem.* **1990**, *9*, 307.

(10) Fendler, J. H. *Membrane Mimetic Chemistry*; Wiley-Interscience: New York, 1982.

(11) Baglioni, P.; Hu, M.; Kevan, L. *J. Phys. Chem.* **1990**, *94*, 2586.

(12) Colaneri, M. J.; Kevan, L.; Thompson, D. H. P.; Hurst, J. K. *J. Phys. Chem.* **1987**, *91*, 4072.

(13) Hu, M.; Kevan, L. *J. Phys. Chem.* **1990**, *94*, 5348.

(14) Bratt, P.; Kang, Y.; Kevan, L.; Nakamura, H.; Matsuo, T. *J. Phys. Chem.* **1991**, *95*, 6399.

(15) Sakaguchi, M.; Kevan, L. *J. Phys. Chem.* **1989**, *93*, 6039.

(16) Sakaguchi, M.; Kevan, L. *J. Phys. Chem.* **1991**, *95*, 5996.

(17) Costa, S. M. B.; Aires/de/Barros, M. R.; Conde, J. P. *J. Photochem.* **1985**, *28*, 153.

(18) Lanot, M. P.; Kevan, L. *J. Phys. Chem.* **1989**, *93*, 998.

(19) Szajdzinska-Pietek, E.; Maldonado, R.; Kevan, L. *J. Am. Chem. Soc.* **1985**, *107*, 6467.

(20) Baglioni, P.; Rivara-Minten, E.; Kevan, L. *J. Phys. Chem.* **1988**, *92*, 4726.

(21) Wang, Y. Y.; Hancock, A. J.; Jean, Y. C. *J. Am. Chem. Soc.* **1983**, *105*, 7272.

(22) Guilard, R.; Senglet, N.; Liu, Y. H.; Sazch, D.; Finsen, E.; Faure, D.; Courieres, T. D.; Kadish, K. M. *Inorg. Chem.* **1991**, *30*, 1898.

(23) Okuno, Y.; Ford, W. E.; Calvin, M. *Synthesis* **1980**, *7*, 537.

(24) Lim, Y. Y.; Fendler, J. H. *J. Am. Chem. Soc.* **1979**, *101*, 4023.

TABLE I: Absorption Maxima (λ_{\max}) for the Visible Bands of H_2PC_9 Solubilized in Various Media

solvent	dielectric constant ^a	optical absorption data: λ_{\max} (nm) ^b				
		SORET	Q (IV)	Q (III)	Q (II)	Q (I)
DODAC		423	517	554	590	648
DHP		421	520	558	593	648
toluene	2.38	423	516	554	590	649
CHCl ₃	4.81	418	519	564	589	649
dichloro-methane	9.08	418	519	564	589	651
ethanol	24.3	416	514	553	588	646
methanol	32.63	416	514	553	588	645

^a Reference 25. ^b ± 0.5 nm.

bubbled with a flow of argon for 10 min, and then the solution was sonicated using a Fisher Model 300 sonic dismembrator with a 4-mm o.d. microtip. The sonication was carried out at 55 ± 3 °C under nitrogen for 15 min or until the solution was no longer turbid.²⁴ The vesicle solution was used immediately after cooling to room temperature. Above a concentration of 0.4 mM, the alkylporphyrins could not be solubilized completely in the vesicle solution. This was observed for each solution with a concentration greater than 0.4 mM as indicated by turbidity remaining after sonication. Vesicular solutions of DHP were prepared following a modified literature procedure.¹² Using the DHP and alkylporphyrin stock solutions, a thin film of DHP and porphyrin was formed in a centrifuge tube. The thin film was dissolved at 72 °C in 1 mL of Tris buffer solution, which consisted of a 20 mM Tris solution adjusted to pH 7.8 with hydrochloric acid. A flow of argon was bubbled for 10 min through the DHP/porphyrin solution, which was then sonicated at 72 ± 4 °C under nitrogen during two 10-min periods separated by a 10-min rest period. Above a concentration of 0.6 mM, the alkylporphyrins could not be solubilized completely in the DHP vesicle solution as indicated by retention of turbidity.

TBBQ dissolved in chloroform was added to the porphyrin/surfactant mixture before formation of the thin film, and then the normal procedures to prepare the vesicle solutions were pursued. $K_3Fe(CN)_6$ was solubilized in either triply distilled water or Tris buffer and then was added to the surfactant solutions just before sonication allowing the $K_3Fe(CN)_6$ to be solubilized in the water pool inside the vesicle, as well as in the bulk solution. Vesicle solutions containing an electron acceptor were prepared with surfactant and porphyrin concentrations of 10 and 0.2 mM, respectively, and with acceptor concentrations ranging from 0 to 1.8 mM.

Photoirradiation and ESR. After preparation, 50 mL of vesicle solution was directly transferred into 2 mm i.d. \times 3 mm o.d. Suprasil quartz tubes, which were sealed at one end and frozen rapidly at 77 K by plunging the tubes into liquid nitrogen. The sample tubes were stored in liquid nitrogen until use. Irradiation of the DODAC solutions containing porphyrin occurred at 77 K with a 300-W Cermax xenon lamp (LX 300UV) and with a power supply from ILC Technology. The irradiation light passed through a 10-cm water filter, and a Corning no. 5030 glass filter for blue light ($320 \text{ nm} < \lambda_{\text{irr}} < 580 \text{ nm}$). The samples were irradiated in liquid nitrogen in a quartz dewar that was rotating during the process to ensure even irradiation of the sample. Electron spin resonance spectra were recorded at 77 K at X-band with a Bruker ESP 300 ESR spectrometer with 100-kHz field modulation and 0.2-mW microwave power.

Results

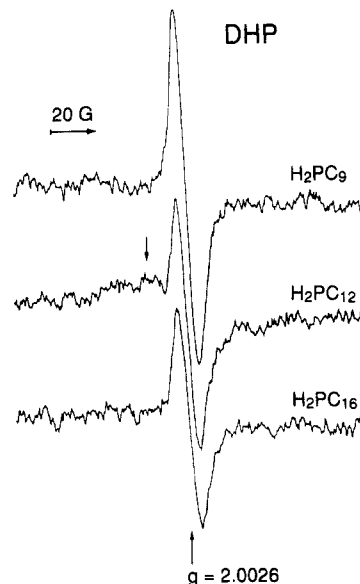
Absorption Spectroscopy Studies. Tables I–III show the absorption maxima (λ_{\max}) for the Soret and Q bands of H_2PC_9 , H_2PC_{12} , and H_2PC_{16} respectively, in DODAC and DHP as well as in toluene, dichloromethane, methanol, and other solvents. The dielectric constants of the solvents²⁵ (characteristic of their polarity) are also given.

TABLE II: Absorption Maxima (λ_{\max}) for the Visible Bands of H_2PC_{12} Solubilized in Various Media

solvent	dielectric constant ^a	optical absorption data: λ_{\max} (nm) ^b				
		SORET	Q (IV)	Q (III)	Q (II)	Q (I)
DODAC		423	521	559	596	649
DHP		421	521	560	594	649
toluene	2.38	423	518	556	590	649
dichloro-methane	9.08	417	517	567	588	651
ethanol	24.63	416	514	552	589	646

^a Reference 25. ^b ± 0.5 nm.**TABLE III: Absorption Maxima (λ_{\max}) for the Visible Bands of H_2PC_{16} Solubilized in Various Media**

solvent	dielectric constant ^a	optical absorption data: λ_{\max} (nm) ^b				
		SORET	Q (IV)	Q (III)	Q (II)	Q (I)
DODAC		423	518	555	591	648
DHP		421	520	559	593	649
toluene	2.38	423	518	556	591	648
dichloro-methane	9.08	418	519	565	589	653
ethanol	24.63	416	514	554	588	646

^a Reference 25. ^b ± 0.5 nm.**Figure 1.** ESR spectra at 77 K of $H_2PC_9^{+}$, $H_2PC_{12}^{+}$, and $H_2PC_{16}^{+}$ in 0.2 mM H_2PC_n and 10 mM DHP vesicle solutions after 15-min photoirradiation.

Photoionization in the Absence of Added Electron Acceptors.

Photoirradiation of frozen DODAC or DHP vesicular solutions not containing any additional substrate did not produce an ESR signal. Photoirradiation of these vesicular solutions containing an alkylporphyrin yielded at 77 K a single symmetrical ESR signal at $g = 2.0026$ with a 7 G line width. The line width and g value of the observed ESR signal were independent of the porphyrin alkyl chain length, and only the signal intensity varied. This signal is attributed to the porphyrin π -radical cation $H_2PC_n^{+}$ described by Fajer and Davis.²⁶ Figure 1 shows the ESR signals of $H_2PC_n^{+}$ in DHP. Similar ESR spectra were obtained in DODAC. In addition to the symmetric signal in the spectra of Figure 1, there is a weak underlying pattern, which shows random variations of intensity in the various porphyrin systems. This weak underlying species most likely corresponds to a radical impurity produced during the sonication process. As observed in Figure 1, this weak pattern does not contribute significantly to the ESR spectrum. A similar nonreproducible pattern has been observed in photo-

(25) Wheat, R. C. *Handbook of Chemistry*, 3rd ed.; CRC: Boca Raton, FL, 1983; p E-51.(26) Fajer, J.; Davis, M. S. In *The Porphyrins*; Dolphin, D., Ed.; Academic: New York, 1978; Vol. IV, Chapter 4.

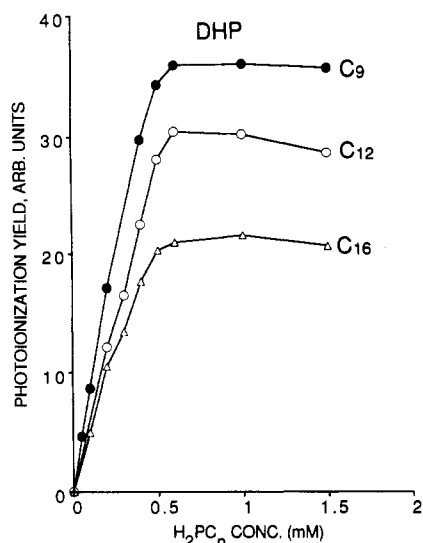


Figure 2. Dependence of $H_2PC_9^{+}$, $H_2PC_{12}^{+}$, and $H_2PC_{16}^{+}$ photoionization yields at 77 K on the H_2PC_n concentration in frozen 10 mM DHP vesicle solutions.

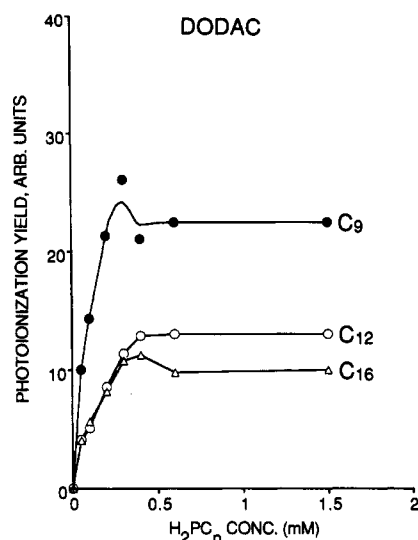


Figure 3. Dependence of $H_2PC_9^{+}$, $H_2PC_{12}^{+}$, and $H_2PC_{16}^{+}$ photoionization yields on the H_2PC_n concentration in frozen 10 mM DODAC vesicle solutions.

irradiated frozen solutions of tetramethylbenzidine (TMB) or alkylviologens in micelles and vesicles.^{6,12,27,28} The intensity of the ESR signal is proportional to the amount of photoproducted porphyrin radical cations in the vesicle solution. Therefore by measuring this intensity it is possible to estimate a relative yield of photoionization. This intensity is measured by double-integrating the ESR signal.

The $H_2PC_n^{+}$ yield increases with irradiation time linearly to about 15 min and then slowly reaches a plateau after about 60 min. The shape of the ESR spectrum does not vary over this time range. An irradiation time of 15 min yields an adequate ESR signal intensity for all systems, and this time is used for all experiments.

The $H_2PC_n^{+}$ yields at 15-min irradiation in DHP and DODAC vesicles are plotted in Figures 2 and 3 as a function of porphyrin concentration. The same vertical scale is used for both figures. Each point is an average of three experiments. The experimental error, determined as the standard deviation, is always between $\pm 9\%$ and $\pm 4\%$ for DODAC and DHP, respectively. In both DODAC and DHP systems, the photoionization yields increase linearly with increasing concentration until they reach a plateau

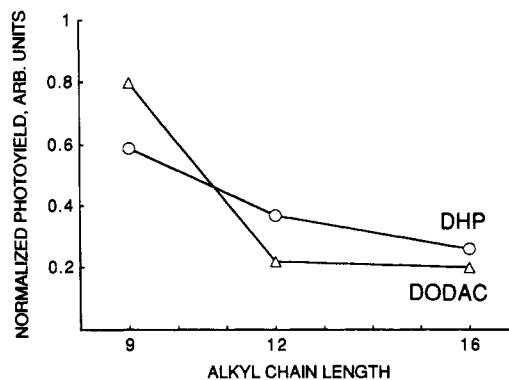


Figure 4. $H_2PC_n^{+}$ photoionization yields at 77 K in frozen 10 mM cationic DODAC and 10 mM anionic DHP vesicle solutions versus alkyl chain length.

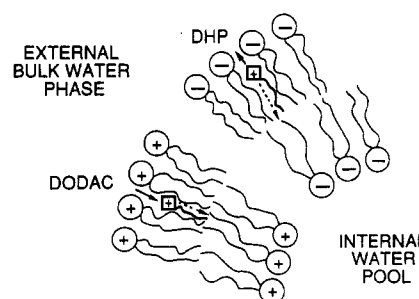


Figure 5. Schematic representation of the relative location of H_2PC_n ($n = 9, 12,$ and 16) in DODAC and DHP vesicles, where the plain arrow represents the electrostatic interactions and the dashed arrow represents the alkyl chain length effect.

value at about 0.4 mM in DODAC and about 0.6 mM in DHP. These limiting concentrations reflect the solubility limit of H_2PC_n in the vesicle suspensions. It is observed that for each alkyl chain length, the maximum $H_2PC_n^{+}$ yields are higher in anionic DHP than in cationic DODAC vesicles. The larger yields in anionic DHP vesicles are at least partially due to the 50% greater solubility of H_2PC_n in DHP versus DODAC vesicle solutions. Therefore, the comparison of the yields as a function of the alkyl chain length is done by taking the initial slopes of the photoyields versus the H_2PC_n concentration. Figure 4 shows these relative $H_2PC_n^{+}$ yields in DODAC and DHP vesicles plotted against the porphyrin alkyl chain length. The vertical scale, which corresponds to the initial slopes of the curves in Figures 2 and 3, is normalized to the initial slope of H_2PC_9 in DODAC vesicle solution.

Photoionization in the Presence of Added TBBQ as an Electron Acceptor. Before irradiation at 77 K of DODAC or DHP vesicle suspensions containing H_2PC_n and TBBQ as an electron acceptor, a nearly symmetrical singlet ESR signal is observed at $g = 2.0088$, which corresponds to the TBBQ anion radical, $TBBQ^{\cdot-}$.²⁹ This dark signal, which increases with increasing $[TBBQ]/[H_2PC_n]$ ratio, must be produced by chemical reaction during the vesicle solution preparation since no signal is observed for TBBQ in dichloromethane. A similar dark signal has been observed for TBBQ in DPPC vesicle suspensions containing ZnTPP.³⁰ After irradiation at 77 K of DHP and DODAC vesicles containing H_2PC_n and TBBQ, an asymmetric singlet ESR signal is observed. This is the superposition of the ESR signal of $TBBQ^{\cdot-}$ at $g = 2.0088$ and the ESR signal of $H_2PC_n^{+}$ at $g = 2.0026$. The signal corresponding to the TBBQ radical anion was subtracted from the total spectrum to obtain the difference spectrum due to $H_2PC_n^{+}$, and its intensity is measured by double integration.

Figures 5 and 6 show the $H_2PC_n^{+}$ yield plotted against the $[TBBQ]/[H_2PC_n]$ ratio in DHP and DODAC vesicles, respectively. Each point is an average of up to four experiments. The experimental error, determined as the standard deviation, was always $\pm 5\%$. As is illustrated in Figure 5, the $H_2PC_n^{+}$ yield in

(27) Narayana, P. A.; Li, A. S. W.; Kevan, L. *J. Am. Chem. Soc.* **1981**, *103*, 3603.

(28) Li, A. S. W.; Kevan, L. *J. Am. Chem. Soc.* **1983**, *105*, 5752.

(29) Hiff, T.; Kevan, L. *Photochem. Photobiol.* **1988**, *48*, 553.

(30) Lanot, M. P.; Kevan, L. *J. Phys. Chem.* **1989**, *93*, 5280.

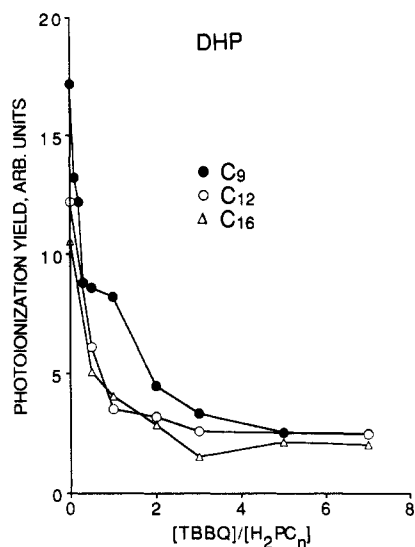


Figure 6. Dependence of $\text{H}_2\text{PC}_9^{+\bullet}$, $\text{H}_2\text{PC}_{12}^{+\bullet}$, and $\text{H}_2\text{PC}_{16}^{+\bullet}$ photoionization yields at 77 K on the $[\text{TBBQ}]/[\text{H}_2\text{PC}_n]$ ratio in frozen 2 mM H_2PC_n and 10 mM DHP vesicle solutions.

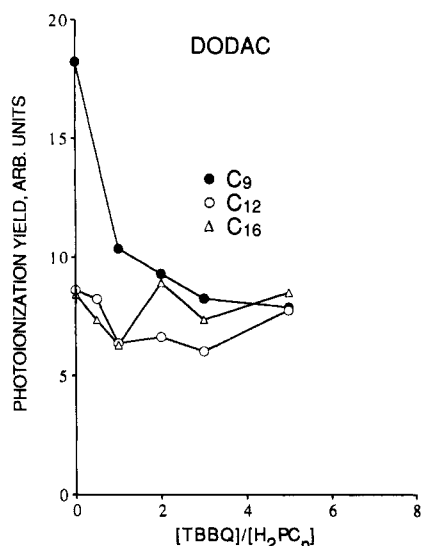


Figure 7. Dependence of $\text{H}_2\text{PC}_9^{+\bullet}$, $\text{H}_2\text{PC}_{12}^{+\bullet}$, and $\text{H}_2\text{PC}_{16}^{+\bullet}$ photoionization yields at 77 K on the $[\text{TBBQ}]/[\text{H}_2\text{PC}_n]$ ratio in frozen 2 mM H_2PC_n and 10 mM DODAC vesicle solutions.

DHP vesicles decreases as the TBBQ concentration increases. The maximum magnitude of decrease of the $\text{H}_2\text{PC}_n^{+\bullet}$ yield upon addition of TBBQ ranges from 85% to 80% depending on the length of the alkyl chain. A similar decrease is obtained in DODAC vesicles for H_2PC_9 , but not for H_2PC_{12} and H_2PC_{16} (Figure 6). The maximum magnitude of decrease is about 55% for $\text{H}_2\text{PC}_9^{+\bullet}$, which is substantially less than in DHP vesicles.

Photoionization in the Presence of Added $\text{K}_3\text{Fe}(\text{CN})_6$ as an Electron Acceptor. Figures 7 and 8 show the dependence of the $\text{H}_2\text{PC}_n^{+\bullet}$ yield on the $[\text{K}_3\text{Fe}(\text{CN})_6]/[\text{H}_2\text{PC}_n]$ ratio in DHP and DODAC vesicles. Each point is an average of up to four experiments. The experimental error, determined as the standard deviation, was always $\pm 5\%$. It is observed that the photoyield decreases as the $[\text{K}_3\text{Fe}(\text{CN})_6]/[\text{H}_2\text{PC}_n]$ ratio increases. In DHP vesicles, the maximum magnitudes of decrease of the $\text{H}_2\text{PC}_n^{+\bullet}$ yield upon addition of $\text{K}_3\text{Fe}(\text{CN})_6$ are 83%, 68%, and 49% for H_2PC_9 , H_2PC_{12} , and H_2PC_{16} , respectively, whereas in DODAC vesicles the maximum magnitudes of decrease of the photoyield for H_2PC_9 , H_2PC_{12} , and H_2PC_{16} are 57%, 44%, and 48%, respectively.

Discussion

Absorption Spectroscopy. Free base porphyrins show a characteristic five-band visible spectrum.³¹ Four Q bands of moderate

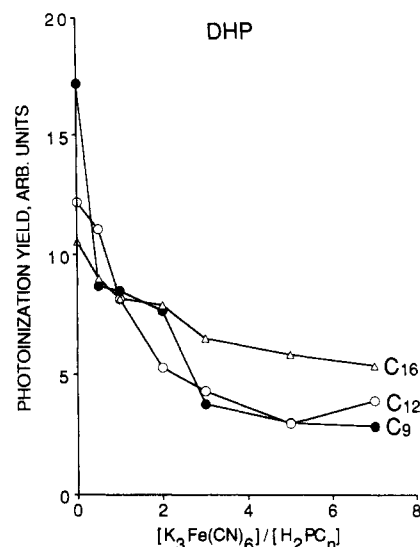


Figure 8. Dependence of $\text{H}_2\text{PC}_9^{+\bullet}$, $\text{H}_2\text{PC}_{12}^{+\bullet}$, and $\text{H}_2\text{PC}_{16}^{+\bullet}$ photoionization yields at 77 K on the $[\text{K}_3\text{Fe}(\text{CN})_6]/[\text{H}_2\text{PC}_n]$ ratio in frozen 2 mM H_2PC_n and 10 mM DHP vesicle solutions.

intensity appear between 500 and 660 nm and an intense Soret band absorbs about 400 nm.³² The positions of these absorption bands are sensitive to the polarity and electron-donating power of the solvent.³³ The spectrum thus indicates the location of alkylporphyrins within a vesicular solution since a vesicle has solubilization sites of different polarities.

The results shown in Tables I–III confirm that the positions of the absorption bands depend on the nature of the solvent. For each alkylporphyrin the λ_{max} values obtained in DODAC vesicles are almost identical to those in toluene which clearly indicates that the polar environment of the alkylporphyrins in DODAC vesicles is very similar to that in toluene.

For DHP vesicles the results are not as clear. However, toluene gives the best match, which suggests that the alkylporphyrins are solubilized in a nonpolar region of DHP vesicles, but presumably in a region more polar than in DODAC vesicles, i.e., relatively closer to the surface. In DODAC vesicles, the positively charged porphyrin rings are electrostatically repelled from the positive vesicle interface, and are "pushed" deeper into the nonpolar region. Conversely, in DHP vesicles the positively charged porphyrins are electrostatically attracted to the negative vesicle interface. Thus in DHP vesicles the porphyrin chromophores are expected to be localized relatively closer to the vesicle interface than in DODAC vesicles. It is generally concluded that organic molecules in vesicles solubilize inside the hydrophobic region near the interface of the vesicle.³⁴

Chromophores bearing a long alkyl chain, such as alkylmethylviologens, are found to solubilize with their polar head at the vesicle surface with their alkyl chain embedded among the hydrophobic surfactant chains.¹² No change in the visible spectra for the different alkylporphyrins solubilized in the vesicles indicates that the differences are too small to distinguish by visible absorption. The photoyield data discussed below supports the existence of significant alkyl chain length effects.

Photoionization in the Absence of Added Electron Acceptors. The most interesting results are given in Figure 4. Four points need to be explained. (1) There is an overall decrease in photoyield as the alkyl chain increases. (2) The photoyield decreases monotonically with increasing alkyl chain length in DHP vesicles, whereas in DODAC vesicles from H_2PC_9 to H_2PC_{12} the photoyield decreases, then remains about constant between H_2PC_{12} and

(31) Gouterman, M. *J. Mol. Spectrosc.* **1951**, *6*, 138.

(32) Gouterman, M. In *The Porphyrins*; Dolphin, D., Ed.; Academic: New York, 1978; Vol. III, Chapter 1.

(33) Phillips, J. N. *Comprehensive Biochemistry*; Elsevier: New York, 1963; p 58.

(34) Thomas, J. K. *The Chemistry of Excitation at Interfaces*; ACS Monograph 181; American Chemical Society: Washington, D.C., 1984; p 245.

H₂PC₁₆. (3) The magnitude of decrease between H₂PC₉ and H₂PC₁₂ is significantly greater in DODAC than in DHP vesicles. (4) The photoyield is higher for H₂PC₉ in DODAC than in DHP vesicles, but for H₂PC₁₂ and H₂PC₁₆ the yield is higher in DHP than in DODAC vesicles. Factors to be taken into account include the charge of the vesicle interface, the charge of the solute, and the location of the solute relative to the vesicle interface.

The decreasing photoyield with increasing alkyl chain length indicates that the ejection of an electron from the porphyrin ring into the bulk water phase across the vesicle interface becomes less effective with longer alkyl chains. The trend in Figure 4 implies that the porphyrin-to-interface distance increases as the alkyl chain is lengthened. The most likely explanation for this behavior is that increasing the alkyl chain length imparts more lipophilicity to the alkylporphyrins which in turn leads to deeper solubilization inside the hydrocarbon core of the vesicle. Analogous behavior has been observed for a series of alkylphenothiazines solubilized in micelle¹¹ and vesicle³⁵ solutions. Such location control of a chromophore in vesicles has been demonstrated previously for dicationic alkylmethylviologens solubilized in DHP¹² and DODAC¹⁶ vesicles. Evidence for deeper solubilization of the chromophore with longer alkyl chains was obtained by electron spin echo modulation (ESEM) measurements, which showed that the deuterium modulation depth decreases as the alkyl chain length increases, indicating that the chromophore is located in a less hydrated region with longer alkyl chains. This alkyl chain length effect is evident in DHP vesicles, where the photoyield decreases almost linearly as the alkyl chain length increases. In DODAC vesicles, however, the decrease in photoyield is only significant from H₂PC₉ to H₂PC₁₂, and between H₂PC₁₂ and H₂PC₁₆, the photoyield is about constant. Thus, H₂PC₁₂ and H₂PC₁₆ are concluded to be at about the same distance from the DODAC vesicle interface.

The electrostatic interaction between the charged porphyrin and the charged surface of the vesicle also plays an important role in affecting the photoyield and explains the differences in photoyields between the DHP and DODAC systems. The optical absorption data indicate that the positively charged porphyrins are localized relatively closer to the interface in anionic DHP than in cationic DODAC vesicles. It appears that the positive surface of the DODAC vesicle, by repelling the positively charged porphyrin, enhances the alkyl chain length effect. Conversely, for the anionic DHP vesicles, the positively charged porphyrin is attracted to the vesicle surface, which attenuates the tendency toward deeper solubilization caused by longer alkyl chains. This electrostatic effect explains why the decrease of the photoyield from H₂PC₉ to H₂PC₁₂ is larger in DODAC than in DHP vesicles. The combined electrostatic and alkyl chain length effects should cause H₂PC₁₆ to be solubilized deeper into the bilayer of the cationic DODAC vesicle than is H₂PC₁₂, but this is not observed. The porphyrin headgroup may be too polar or too bulky to be pulled into the hydrocarbon core too much.³⁶ In DHP vesicles, the alkyl chain effect is weakened by the electrostatic effect; therefore, the porphyrins are located closer to the surface and are pulled into the vesicle to a lesser extent than in DODAC vesicles. In this case, H₂PC₁₆ penetrates deeper than H₂PC₁₂ into DHP vesicles. This electrostatic effect also has been demonstrated for a series of anionic alkylphenothiazine derivatives in anionic and cationic vesicles where it was found by ESEM that the anionic phenothiazine moiety is located in a more hydrophobic region in anionic DHP than in cationic DODAC vesicles.³⁵ The combined alkyl chain length and electrostatic effects on alkylporphyrin location in DHP and DODAC vesicles are summarized in Figure 5.

Recent studies^{14,18} at 77 K in frozen micelles and vesicles of different surface charge have demonstrated that the escape of the electron from the irradiated species to the bulk phase is enhanced

by more positively charged vesicle surfaces. For instance, it was observed³⁷ that the photoyield of ZnTPP is 50% greater in positively charged DODAC than in neutral (actually zwitterionic) dipalmitoylphosphatidylcholine (DPPC) and is 70% less in negatively charged DHP-DPPC vesicles than in positively charged DODAC vesicles. This effect of the vesicle surface charge on the photoyield can account for the higher H₂PC₉^{•+} yield in cationic DODAC than in anionic DHP vesicles. However for H₂PC₁₂ and H₂PC₁₆ the charge effect on the photoyields seems less important than the porphyrin-to-vesicle surface distance. Porphyrins with alkyl chains of 12 or 16 carbons are located closer to the interface in DHP than in DODAC vesicles. This enhances the electron escape across the interface regardless of its charge and gives higher photoyields in the anionic DHP vesicle over the cationic DODAC vesicle.

Photoionization in the Presence of Added Electron Acceptors. The fact that the intensity of the H₂PC_n^{•+} and TBBQ⁻ ESR signals are affected by variations of the [TBBQ]/[H₂PC_n] ratio indicates that photoirradiation produces electron transfer from the alkylporphyrin to the quinone. TBBQ is an electron acceptor, but a decreasing H₂PC_n^{•+} yield with increasing TBBQ concentration indicates that back electron transfer from the quinone radical anion to the porphyrin is dominant. The explanation for this trend is that increasing the TBBQ concentration causes an effective decrease in the mean TBBQ/H₂PC_n distance, which enhances the efficiency of the back electron transfer.³⁸ The magnitude of the decrease in the ESR signal with added acceptor gives an indication as to the relative importance of back electron transfer.

As observed in Figure 6, in the DHP system, the decrease of the H₂PC_n^{•+} yield upon addition of TBBQ is 80–85%, indicating that back electron transfer is very effective. This drop in photoyield suggests that H₂PC_n and TBBQ are localized close together near the interface. Comparatively, the decrease of the photoyield upon addition of TBBQ is 1.5 times weaker in DODAC (Figure 7) than in DHP vesicles since the maximum decrease in photoyield for H₂PC₉ is 55%. This difference indicates that in DODAC vesicles, H₂PC₉ is not located as close to TBBQ as it is in DHP vesicles. For H₂PC₁₂ and H₂PC₁₆ solubilized in DODAC vesicles, there is essentially no decrease in photoyield as the [TBBQ]/[H₂PC_n] ratio increases. Back electron transfer is, therefore, even less important than with H₂PC₉. Thus, in DODAC vesicles, H₂PC₁₂ and H₂PC₁₆ are located further from TBBQ than is H₂PC₉. H₂PC₁₂ and H₂PC₁₆ are probably near the same distance from TBBQ and therefore from the surface, since they show the same trend.

In DHP vesicles, the general trend observed in Figure 7 is a decrease of the H₂PC_n^{•+} yield with increasing [K₃Fe(CN)₆]/[H₂PC_n] ratio. This trend is indicative of back electron transfer from Fe(CN)₆⁴⁻ to the alkylporphyrin radical across the vesicle interface. The extent of decrease in the photoyield of H₂PC_n^{•+} upon addition of K₃Fe(CN)₆ to a vesicle suspension not containing any electron acceptors is directly related to the efficiency of the back electron transfer from Fe(CN)₆⁴⁻ to the porphyrin radical. This trend in the magnitude of decrease implies that the efficiency of the back electron transfer decreases with increasing porphyrin alkyl chain length. The rate of back electron transfer is critically dependent on the donor-acceptor distance.³⁸ The decrease in back electron transfer is thus consistent with earlier observations that as the alkyl chain increases, the porphyrins are solubilized deeper within the vesicle and hence further from the interface.

Figure 9 shows that in DODAC vesicle the H₂PC_n^{•+} yield decreases with increasing [K₃Fe(CN)₆]/[H₂PC_n] ratio. This trend is indicative of back electron transfer from Fe(CN)₆⁴⁻ to the alkylporphyrin radical across the vesicle interface. In this case, however, the decrease of the photoyield caused by this back electron transfer is less than that observed for the same experiment using DHP vesicles. This difference results from the fact that the porphyrins are located deeper inside the vesicle in DODAC

(35) Sakaguchi, M.; Hu, M.; Kevan, L. *J. Phys. Chem.* **1990**, *94*, 870.

(36) March, D.; Watts, A. In *Liposomes: From Physical Structure to Therapeutic Applications*; Knight, C. G., Ed.; Elsevier: Amsterdam, 1981; Chapter 6.

(37) Lanot, M. P. M.S. Thesis, University of Houston, 1988.

(38) Dexter, D. L. *J. Phys. Chem.* **1953**, *21*, 836.

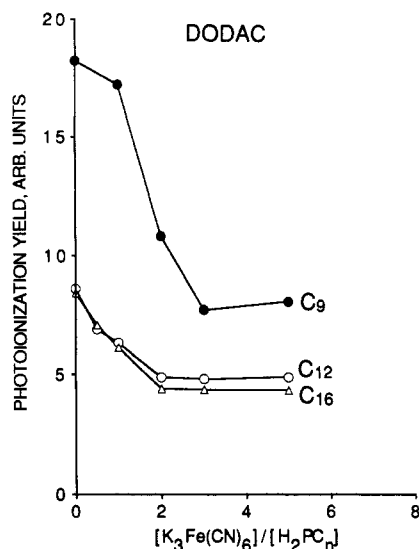


Figure 9. Dependence of $\text{H}_2\text{PC}_9^{++}$, $\text{H}_2\text{PC}_{12}^{++}$, and $\text{H}_2\text{PC}_{16}^{++}$ photoionization yields at 77 K on the $[\text{K}_3\text{Fe}(\text{CN})_6]/[\text{H}_2\text{PC}_n]$ ratio in frozen 2 mM H_2PC_n and 10 mM DODAC vesicle solutions.

than in DHP. In particular, the photoyield decreases from H_2PC_9 to H_2PC_{12} and then remains constant. This variation in the trend is consistent with the observation that both H_2PC_{12} and H_2PC_{16} are solubilized at a similar distance from the interface, but further inside the vesicle than H_2PC_9 .

Since back electron transfer seems prevalent in the presence of electron acceptors, let us consider what might be predicted from simple electrostatics. In anionic DHP vesicles, the negatively charged $\text{Fe}(\text{CN})_6^{3-}$ ion should be repelled from the anionic interface into the bulk phase, whereas the potassium cation should be attracted to the surface. On the basis of this simple electrostatic model, the $\text{Fe}(\text{CN})_6^{3-}$ should be located far enough from the porphyrin to preclude strong back electron transfer. Also back electron transfer is kinetically unfavorable due to the electrostatic barrier provided by the anionic DHP interface. However, the observation of back electron transfer suggests that a simple electrostatic model is not valid to describe the complexity of the DHP interface containing $\text{K}_3\text{Fe}(\text{CN})_6$ and porphyrins. Partial neutralization of the negatively charged DHP vesicle surface by potassium cations may enhance back electron transfer. It has been shown that adding salt to a vesicle or micelle solution can affect the photoyield.^{39,40} Similarly, back electron transfer has been observed from $\text{Fe}(\text{CN})_6^{4-}$ to the TMB radical cation solubilized in an anionic micelle.⁴¹ This back electron transfer was attributed to partial neutralization of the ionic micellar interface. In DODAC vesicles, the negatively charged $\text{Fe}(\text{CN})_6^{3-}$ ions should be attracted to the positively charged interface of the vesicle. There, a simple electrostatic model seems consistent with the occurrence of back electron transfer, since then the ferricyanide ions are expected to be located at the interface. The photoyield results obtained with the addition of $\text{K}_3\text{Fe}(\text{CN})_6$ to both DHP and DODAC vesicles support the relative locations determined for the

alkylporphyrins inside the bilayer of the DHP and DODAC vesicles.

Conclusions

The location of a series of three alkyl porphyrins (H_2PC_n , $n = 9, 12, 16$) within DODAC and DHP vesicles was investigated by optical absorption spectroscopy. The positions of the porphyrin absorption bands are dependent on the polarity of the solubilization medium. By using solvents of known polarity as references, the porphyrins are found to be solubilized in a nonpolar environment of the vesicles. This result indicates that the porphyrins are anchored among the hydrocarbon chains of the surfactant molecules with the porphyrin ring pointing toward the vesicle interface. The results also show that the porphyrins are solubilized closer to the interface in DHP than in DODAC vesicles. ESR studies of photoirradiated DODAC and DHP vesicle solutions confirm these results and provide insight as to the location of the porphyrins in these systems as a function of the length of their alkyl chains. The overall decrease of the $\text{H}_2\text{PC}_n^{++}$ yield with increasing alkyl chain length indicates that extending the length of the alkyl chain solubilizes the porphyrin moiety deeper within the hydrocarbon core of the DHP and DODAC vesicles. Electrostatic interactions between the porphyrin and the vesicle interface account for specific differences in the $\text{H}_2\text{PC}_n^{++}$ yields between the DODAC and DHP systems. The positive surface of the DODAC vesicle, which repels the positively charged porphyrin, enhances the alkyl chain length effect. Conversely, in the anionic DHP vesicle, the alkyl chain length effect is weakened because the positively charged porphyrins are attracted to the cationic DHP surface. Thus, in anionic DHP vesicles the cationic porphyrins are located closer to the surface than in cationic DODAC vesicles. The relative porphyrin-to-vesicle interface distances are deduced to be $\text{H}_2\text{PC}_9 < \text{H}_2\text{PC}_{12} < \text{H}_2\text{PC}_{16}$ in DHP vesicles, and $\text{H}_2\text{PC}_9 < \text{H}_2\text{PC}_{12} \approx \text{H}_2\text{PC}_{16}$ in DODAC vesicles. This work demonstrates that effective location control of an electron donor in photoinduced charge separation across a surfactant assembly interface can be achieved by combining an alkyl chain length effect of the solute and an electrostatic effect between the donor molecule and the vesicle surface. These results are supported by an ESR study of photoionized alkylporphyrins solubilized in DHP and DODAC vesicle solutions in the presence of TBBQ and $\text{K}_3\text{Fe}(\text{CN})_6$ as electron acceptors. Upon addition of either acceptor to the DHP or DODAC systems, the photoyield generally decreased with increasing acceptor concentration indicating that back electron transfer occurred from the acceptor to the alkylporphyrin. The efficiency of back electron transfer is enhanced as the porphyrin-acceptor distance is decreased. The magnitude of the decrease of the $\text{H}_2\text{PC}_n^{++}$ yield upon addition of electron acceptor gives useful insight into the location of the alkylporphyrins relative to the electron acceptor and is consistent with the relative locations deduced in the absence of electron acceptors.

Acknowledgment. This research was supported by the Division of Chemical Sciences, Office of Basic Energy Sciences, Office of Energy Research, U.S. Department of Energy.

Registry No. H_2TPPyP , 69458-21-5; H_2PC_9 , 136676-61-4; H_2PC_{16} , 107407-89-6; H_2PC_{12} , 95245-04-8; H_2TPP , 917-23-7; DODAC, 107-64-2; DHP, 2197-63-9; TBBQ, 488-48-2; $\text{K}_3\text{Fe}(\text{CN})_6$, 13746-66-2; benzaldehyde, 100-52-7; 4-pyridinecarboxaldehyde, 872-85-5; pyrrole, 109-97-7; nonyl bromide, 693-58-3; dodecyl bromide, 143-15-7; hexadecyl bromide, 112-82-3.

(39) Fang, Y.; Tollin, G. *Photochem. Photobiol.* **1983**, *39*, 685.

(40) Hiff, T.; Kevan, L. *J. Phys. Chem.* **1989**, *93*, 3227.

(41) Stenland, C.; Kevan, L. *Radiat. Phys. Chem.* **1991**, *37*, 423.